Journal of Non-Crystalline Solids 120 (1990) 152–171
North-Holland

CHEMICAL PROCESSES IN GLASS POLISHING

Lee M. COOK

Galileo Electro-Optics Corp., Galileo Park, P.O. Box 550, Sturbridge, MA 01566, USA

Chemical processes which occur during glass polishing are reviewed within the context of current mechanical models for the polishing process. The central chemical process which occurs is the interaction of both the glass surface and the polishing particle with water. A detailed mechanico-chemical model for the polishing process is proposed.

1. Introduction

Considerable time has elapsed since the last overview of glass polishing in a glass science forum. The last such review given in the present conference series was in 1976, and the last comprehensive review on the subject is now 10 years old [1]. Since that time, considerable progress has been made in both the technology of polishing and in the understanding of polishing mechanisms.

Much of the coverage of this technology is found in optics and optical engineering publications. These publications are seldom read by the glass scientist because polishing is commonly considered to be a mechanical art rather than a scientific discipline. In reality glass polishing and glass surface science are fundamentally related by their dependence on an understanding of aqueous corrosion chemistry and fracture mechanics processes. The object of this paper is to stimulate interaction between the two communities. To this end, the mechanics of the polishing process and chemical effects in polishing will be reviewed to develop a model for the polishing process. For the sake of brevity, discussion is primarily restricted to fixed-charge pitch polishing of silicate glasses and excludes wholly chemical polishing via HF or other acids.

2. Mechanics of polishing

As reviewed by Izumitani [1] and Holland [2], the mechanisms that have been proposed for polishing over the years may be categorized as mechanical wear, plastic flow, chemical, and mechano-chemical. The mechano-chemical mechanism is generally accepted. The major question at present is whether mechanical or chemical effects are dominant.

2.1. Kinetics

Glass polishing occurs in an aqueous slurry of fine abrasive particles of diameters less than ~ 3 μm. These polishing particles are generally embedded in a viscoelastic material such as pitch, which is mounted on a plate. The pitched plate (the polishing lap) is pressed against the surface to be polished and moves along its surface at a fixed speed. Thus the polishing process may be described as a two-body wear problem, with the polishing grain planing down the surface of the glass. The classic equation for polishing is the Preston equation [3]:

$$\Delta H/\Delta t = K_{\mathrm{P}} * (L/A) * (\Delta s/\Delta t). \quad (1)$$

$\Delta H/\Delta t$ is the change in height H over time t, L is the total load, A the surface area on which wear occurs and Δs is the relative travel between glass surface and lap over which the wear occurs. K_{P} is the Preston coefficient, which is process dependent, with units of $\mathrm{cm}^2/\mathrm{dyn}$. This can be rewritten as

$$\Delta M = \mathrm{d}\, K_{\mathrm{P}} L\, \Delta s, \quad (2)$$

where M is mass and d is glass density. Similar relationships describe most forms of abrasive wear.

The kinetics of polishing are, therefore:

(1) The rate of surface height removal is dependent on pressure, which is determined by the contact area of the surface. As polishing proceeds and contact area approaches the geometrical area of the part, $\Delta H/\Delta t$ decays to some asymptotic value characteristic of the system, as does surface roughness.

(2) The rate of surface removal (or weight loss) increases directly with increasing load and lap velocity.

(3) The rate of surface removal is independent of polishing particle size within some upper limit. No real data exist for a lower size limit.

The constant weight loss allows precise calculation of the Preston coefficient from easily measured and precisely controlled experimental parameters (density, mass change, load and lap velocity). For polishing of silicate glasses, the Preston coefficient is only weakly variant for a given polishing compound. For cerium oxide, typical values of K_P are $\sim 8 \times 10^{-14}$ cm^2/dyn for borosilicates such as BK7 polished on pitch at very low loads and slow rates [4]. Similar values are obtained for ophthalmic crown glasses polished on felt and plastic pads at high speeds and loads [5]. Fused silica, the least chemically reactive glass, yields a K_P of $\sim 2 \times 10^{-14}$ cm^2/dyn.

Uniform local pressure at the point of contact between the polishing grain and the glass surface is largely determined by the nature of the polishing lap. As summarized by Izumitani [1], its function is to hold the polishing particles, transmit load forces to the particle/glass surface and conform precisely to the article being polished. Consequently, all conventional polishing substrates are either viscoelastic, e.g. pitch or plastics, or elastic, e.g. felt or rubber materials. The use of pitch yields the smoothest surfaces and is the best understood substrate. It is a viscous newtonian liquid, with an optimum viscosity of $2\text{–}8 \times 10^9$ P for glass polishing [6]. A model for the settling of polishing particles into the pitch surface is illustrated in fig. 1. For the case of a pitch surface coated with polishing particles of a given size distribution, the full load is initially on the largest particles (fig. 1(b)), which sink rapidly into the pitch following Stokes' law, allowing contact with smaller grains (fig. 1(c)). This settling could reduce the load on the larger particles and, therefore, their rate of penetration. With time, all particles become load bearing, applying uniform force to the glass surface, with a pitch to glass surface gap determined by the diameter of the smallest particle (fig. 1(d)). This is the stage at which superpolishing is thought to occur.

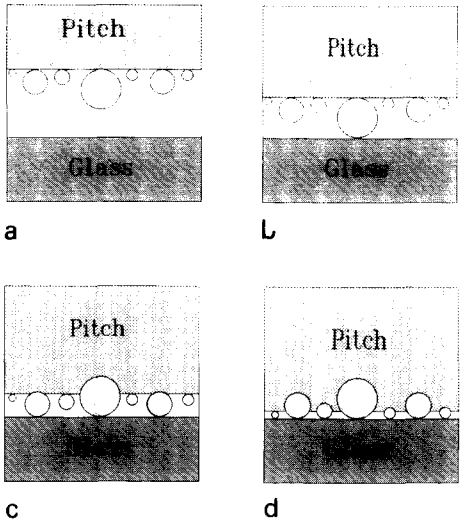

Fig. 1. Function of pitch lap (after ref. [6]). (a) Charged lap prior to contact; (b) first contact loads largest particles, causing them to sink into the pitch; (c) smaller particles are brought into contact; (d) with time, all particles become load bearing.

The mechanics of the interaction between polishing particles and the glass surface can be described (fig. 2) by a model in which a spherical particle of diameter ϕ under uniform load L penetrates the surface with force F and moves along the surface at some velocity, $\Delta s/\Delta t$, removing a glass volume of dimensions proportional to the penetration. This model was first developed by Brown et al. [7] in 1981 for the superpolishing of metals. In 1984, Brown and Cook [8] proposed that the model was equally applicable to glass polishing. More recently, the model has been extended to describe what has been termed ductile grinding in brittle materials (i.e. processes using abrasive particles of sizes below their minimum comminution diameter [9–11].

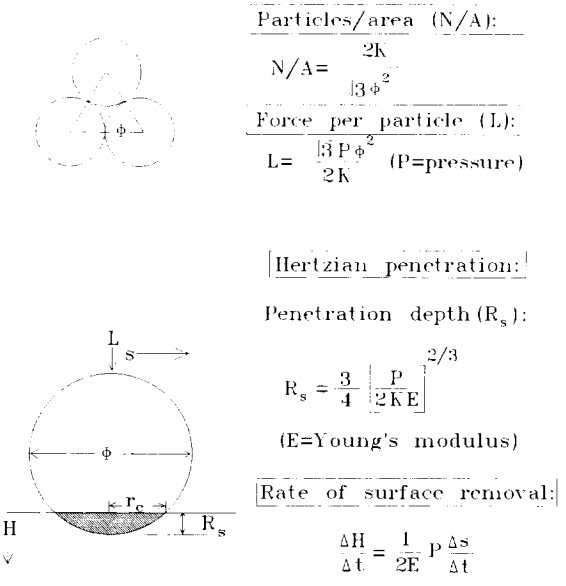

Fig. 2. Mechanics of particle/glass contact (after ref. [7]).

With these assumptions and a standard Hertzian penetration (fig. 2), the rate of surface removal can be expressed as

$$\Delta H/\Delta t = (2E)^{-1} P\,\Delta s/\Delta t. \qquad (3)$$

This is equivalent to the Preston equation as expressed in eq. (1) above, but with the Preston constant expressed as the inverse of twice Young's modulus, E, and pressure, P, replacing load per area. Surface roughness, R_s, is the penetration depth of the particle into the surface, given by

$$R_s = 3/4\phi(P/2kE)^{2/3}, \qquad (4)$$

where k is particle concentration (unity for a fully filled close hexagonal packing).

These polishing kinetics are distinctly different from conventional abrasive grinding due to the independence of rate on abrasive size, and to the differences in dependence of both rate and surface roughness on Young's modulus.

The ductile grinding model generally gives good quantitative fits to experimental data for both rate and roughness for a variety of metals. Brittle materials (SiC, SiO_2, BK7) show a parametric fit. However, the rate constants for glasses were more than an order of magnitude lower than predicted from eq. (4), and were almost half an order of magnitude below the rate constant found for cerium polishing.

Two other techniques have been demonstrated to yield superpolished surfaces whose polishing kinetics are consistent with the model presented above. Float polishing [12] uses a rapidly rotating tin lap with an aqueous polishing slurry of colloidal SiO_2 (4–7 nm). Speeds at the surface of the part being worked are on the order of 80 cm/s, with the part hydrodynamically skating above the surface of the lap on a thin liquid layer. The mechanism proposed for the process is an elastic bombardment of the surface of the part by the polishing grains, leading to contact bonding and removal of weakly bonded atoms from the surface.

A second technique, elastic emission machining (EEM), developed for finishing single crystal semiconductors, uses a large urethane ball that hydrodynamically skates above the surface of the part on an aqueous slurry of submicron polishing compound (0.6 μm SiO_2, Al_2O_3, ZrO_2). The model advanced for this process [13,14] is impingement of particles carried in the turbulent liquid leading to Hertzian penetration of the surface by the particles, converting kinetic energy to strain energy. Local bonding during contact leads to weakening of binding forces at the surface, which allows atomic removal to occur without introducing lattice dislocations. While most EEM work involves semiconductors, it has also been demonstrated to be effective for float glass [13].

It is appropriate to review the physical scale and environment in which the interaction between the polishing particle and glass surface occurs. For the ideal case of polishing a 25 mm diameter plate of SiO_2, use of spherical particles with $\phi = 3$ μm, an abrasive fill fraction $K = 0.5$, a part pressure $P \approx 0.07$ kg/cm^2 and a velocity V_p of 5 cm/s are typical polishing conditions. From eq. (4), one obtains a penetration depth $R_s \approx 0.2$ nm. The most probable physical interactions during polishing are thus confined to the outermost layers of SiO_4 tetrahedra on the glass surface. This degree of penetration is negligible when compared with the radius of the polishing particle (~ 0.01%). Accordingly, just a short radial distance away from the initial point of contact, the glass structure is no longer contiguous with the polishing

particle but is merely overshadowed by it. The small free liquid volume of the system yields extremely high surface/volume ratios, even far away from the polishing particle itself.

2.2. Effects of frictional forces

The maximum tensile stress, σ_t, for the case of a static Hertzian spherical indenter may be calculated [15] from the expression

$$\sigma_t = \tfrac{1}{2}(1-2\nu)\,p_0, \tag{5}$$

where $p_0 = L/\pi r_c^2$ is the mean contact pressure over a circular zone of radius r_c, and ν is Poisson's ratio for the glass. The radius of contact is obtained from

$$r_c = \left\{\tfrac{3}{4}L(\phi/2)\left[(1-\nu^2)/E + (1-\nu'^2)/E'\right]\right\}^{1/3}, \tag{6}$$

where ν' and E' are the Poisson's ratio and Young's modulus of the polishing particle, respectively.

The analytical solution to the travelling indenter problem is well known [15]. Particle movement across the glass surface shifts the subsurface stress fields to give a compressive zone extending outwards from the leading edge and a corresponding tensile zone extending from the trailing edge as illustrated in fig. 3. The maximum tensile stress may be expressed as

$$\sigma_t = (1-2\nu/2)\,p_0(1+A\mu), \tag{7}$$

where μ is the coefficient of friction between the particle and the glass surface and A is a dimensionless parameter

$$A = [3\pi(4+\nu)]/[8(1-2\nu)]. \tag{8}$$

Amontons law defines the coefficient of friction as the frictional force F divided by the load. At the scale of interaction under discussion, an operational definition of the friction force is

$$F = \pi r_c^2 f_b E/10, \tag{9}$$

where πr_c^2 is the contact area between polishing particle and the glass surface, f_b is the fraction of the contact area in which bonding occurs (~ 1%), and $E/10$ is an estimate for the theoretical fracture strength σ_s of network bonds. Thus chemically active polishing particles such as CeO_2, having a large fraction of surface species bonding to the glass, will generate higher frictional forces and higher surface stresses than more inert materials such as diamond.

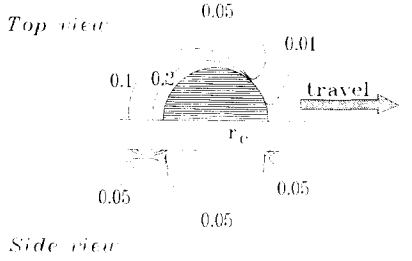

Fig. 3. Half surface view and side view of contours of greatest stress for moving indenter. r_c = contact radius, $\mu = -0.1$, $\nu = 0.33$. Unit of stress is p_0. (After ref. [15].)

For the case given above, σ_t is ~ 300 mPa, or ~ 4% of the intrinsic strength of the bulk glass ($\approx E/10$). Tensile stress varies weakly with particle diameter and load, as expected from eqs. (5) and (6). The ranges of coefficients of friction calculated for a variety of particle diameters and loads (0.15–0.5) are consistent with values which are measured during polishing (0.05–0.8).

From fig. 3 it is apparent that the stress field depths are quite shallow, on the order of the contact radius r_c (i.e. $\approx$ 10 nm). Corresponding hydrostatic pressures should occur in the liquid zone around the leading edge of the polishing particle, falling off rapidly towards the trailing edge. Finally, appreciable heat must necessarily evolve during surface removal ($P\,\Delta V$ work). The magnitude of surface temperatures during polishing has been the subject of considerable debate [2]. It is safe to assume local temperatures of at least 100 °C, increasing as load and particle velocity increase.

2.3. Structural influences on kinetics

Examination of the most extensive collection of polishing rate data for a variety of optical glasses by Izumitani [16] gives polishing rates proportional to $1/E$ (fig. 4). Observed rates, however, were well below those predicted by the mechanical model presented previously. Separate rate curves

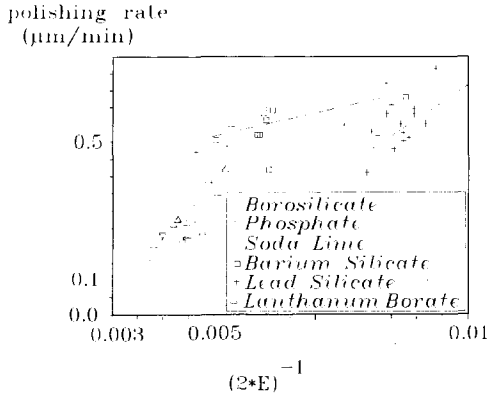

Fig. 4. Polishing rate vs. $1/E$ for a variety of optical glasses (from ref. [16]).

are obtained for lead silicate glasses, barium silicates and lanthanum borates, with slopes increasing with increasing chemical durability. In Izumitani's study, similar relationships were observed for polishing rates versus the microhardness of the leached surface layer and weight loss in water. These similarities indicate a strong influence of surface chemistry and structure on the purely mechanical model presented above.

3. The role of chemistry in polishing

The previous discussion raises a central question. Why are the observed rate constants for glass polishing so much lower than expected? If one accepts the model, then several explanations come to mind.

The penetration volumes calculated from a Hertzian analysis may be too large for two reasons. First, it is recognized that elastic properties at the surface may not be the same as for the bulk material. This is particularly true if there is a reaction with the surroundings. However, the bulk elastic constants of hydrated silicate glasses are not appreciably different from their anhydrous analogs [17,18], suggesting that this effect is relatively minor.

Second, it is also recognized that applied forces may be relieved by inelastic deformation, particularly at the low loadings and penetrations occurring during polishing. The extent of this is hard to quantify, as material constants for the surface itself are not available.

Another explanation is that either a portion of the material in the indentation volume is either not being removed by the abrasive particle or it is being redeposited on the surface.

In support of this last argument, Brown and Cook [8] first proposed the concept of 'tooth' to explain the removal of material in the polishing regime. For both elastic and plastic indentation, wear cannot occur unless net material transport off the worn surface is positive. Otherwise, the material behind the travelling indenter will simply spring back to its original position (elastic effects) or change its topology (plastic effects). At the scale of interaction expected during polishing, material removal will occur in terms of single silica tetrahedra or small multiples thereof. Such removal is on the scale of a chemical process such as dissolution rather than mechanically produced particle generation, as would be expected during grinding.

Mass transport during polishing is determined by the relative rates of the following processes:

(1) movement of solvent into the surface layer under the load imposed by the polishing particle;
(2) surface dissolution under load;
(3) adsorption of dissolution products onto the surface of the polishing particle;
(4) the rate of back-deposition of dissolution products onto the surface;
(5) surface dissolution which occurs between particle impacts.

It is suggested that polishing compounds such as CeO_2 or ZrO_2 possess a chemical tooth that expedites both bond shearing at the glass surface and transport of reaction products away from the surface faster than their rate of redeposition.

For all known polishing compounds, including diamond, glass polishing is critically dependent upon the presence of water. Polishing rates are observed to be near zero in hydrocarbon liquids such as kerosene [19], paraffin [20], or oil [1], as well as in liquids without hydroxyl groups, such as formamide [20]. Surface quality in such liquids is also poor.

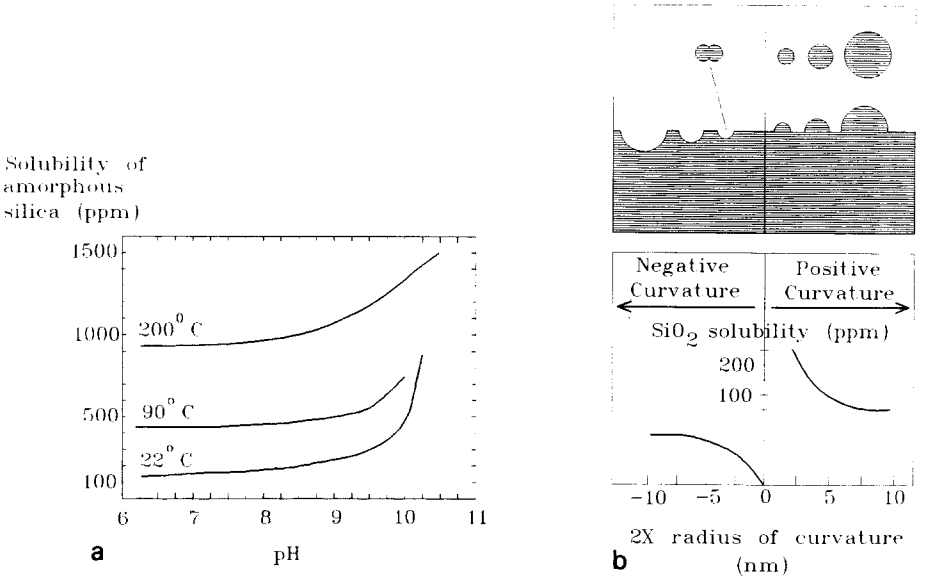

Fig. 5. Data for aqueous solubility of silica glass (from ref. [22]). (a) Equilibrium solubility of silica as a function of pH and temperature. (b) Variation of silica solubility with radius of curvature of surface.

Cornish and Watt [20] reviewed cerium polishing rates relative to water for a series of alcohols ranging from methanol to n-dodecanol. Polishing rates were found to increase directly with increasing hydroxyl reactivity, with water giving by far the highest rate. Similarly, Silvernail and Goetzinger [21] studied cerium polishing rates in a series of ethylene glycol/water mixtures. Polishing rates were extremely low in pure ethylene glycol, increasing logarithmically with the molar concentration of water in solution.

From the above, it is apparent that the interaction of the system with water is the primary chemical process in glass polishing. An understanding of the physicochemical nature of both the glass and polishing compound surfaces in an aqueous environment is central to an understanding of this chemical 'tooth'.

3.1. Water–silica reactions

The reactions between siloxane bonds (Si–O–Si) and water primarily determine the behavior of silicate glass surfaces during polishing, as attack of the siloxane network will control the rate of surface removal. This reaction can be described as a reversible depolymerization reaction [22] whose simplest expression is

$$(SiO_2)_x + 2H_2O \rightleftarrows (SiO_2)_{x-1} + Si(OH)_4. \quad (10)$$

Iler [22] gives a more general expression for the hydration/dehydration process at a surface

$$\left[Si_nO_{2n-(nx/2)}(OH)_{nx}\right] + mSi(OH)_4 \rightleftarrows \left[Si_{n+m}O_{2n-(nx/2)+2m(2-p)}(OH)_{nx+4(m-p)}\right] + 2pmH_2O, \quad (11)$$

where n is the number of silica atoms in a polymer or particle (∞ for the massive solid), x is the number of OH groups per silicon atom in the polymer (<4), m is the number of $Si(OH)_4$ monomers added to the polymer, and p is the fraction of hydroxyl groups per $Si(OH)_4$ that are converted to water during polymerization. When the equilibrium concentration for the monomer is exceeded near a solid silica surface, x is very small, $p = 1$ and n is large; thus, dense silica of relatively low water content precipitates at the silica surface. This type of deposition occurs preferentially at high temperatures and at neutral to alkaline pH, i.e. the surface conditions expected

during polishing. The equilibrium concentration of surface hydroxyls on fully hydrated massive vitreous silica is 4.6/nm^2 [22,23] and increases to ~ 8/nm^2 for silica gels [18]. The hydration reaction is quite slow under ambient conditions, e.g. the equilibrium solution concentration of the monomer for vitreous silica in water at 20 °C is ~ 100 ppm $Si(OH)_4$ [22]. Figure 5(a) shows equilibrium solubility as a function of pH for temperatures of 0–200 °C. One notes that if either the pressure or temperature is suddenly decreased, excess monomer above the new solubility limit is precipitated from solution. Also, fig. 5(b) indicates the effect of particle and surface curvature on the solubility of silica in water.

The surface hydroxyl equilibrium may be described by

$$\equiv Si{-}OH_2^+ \overset{K^1}{\rightleftarrows} \equiv Si{-}OH \overset{K^2}{\rightleftarrows} \equiv Si{-}O^-. \qquad (12)$$

The left species is a Bronsted acid (proton donor) with equilibrium constant K^1 while the right species is a Bronsted base (proton acceptor) with equilibrium constant K^2. For silica, pK^1, is −2, strongly shifting reaction (12) to the right. In the pH range above pK^1 the fraction of Bronsted bases n_b may be calculated via [22]

$$n_b = (10^{5.2\ \log(pH)-4.78})/4.6, \qquad (13)$$

where the denominator is the surface hydroxyl concentration per nm^2. Above pH ≈ 11, the surface hydroxyls are completely dissociated. Equi-molar surface concentrations of each species occur at pH ≈ 9.8, precisely the pH range which yields maximum polishing rates and smoothness for cerium and zirconium compounds. At pH7, the surface concentration of $Si{-}O^-$ is 9% of total hydroxyl. The most rapid network condensation occurs via

$$\equiv Si{\cdot}\cdot O^- + \equiv Si{-}OH \rightleftarrows \equiv Si{-}O{-}Si\equiv + OH^-, \qquad (14)$$

the rate of which is directly proportional to the $Si{-}O^-$ concentration [22]. The fractional area of the particle/glass contact interface that is actually engaged in chemical bonding is used to determine the frictional force in eq. (9) above, and may therefore be related to the concentration of surface anions. For the case of silica polishing silica in water (pH = 7), $n_b = 0.09$. For an ionic OH radius of 0.135 nm, the total hydroxyl density on the fully hydroxylated silica surface equals 26% of the surface area. Thus the fraction of the surface area covered by anions is 2.3%, quite close to the bonded fraction of the contact area used in eq. (9) above.

The reversal of eq. (14) above is the breakage of network forming siloxane bonds by hydroxyl to form a hydrated silica surface. For the case of water, this may be simplified to

$$\equiv Si{-}O{-}Si\equiv + H_2O \rightleftarrows 2\ \equiv Si{-}OH. \qquad (15)$$

The rate of this reaction below the surface is believed to be controlled by the diffusion of water in silica [24]. The diffusion coefficient of water in silica is quite low. Low temperature measurements of the steady state diffusion coefficient yield values of ~ 10^{-19} cm^2/s at ambient and ~ 10^{-18} cm^2/s at 90 °C [25,26]. Lanford et al. [26] used ^{15}N nuclear reaction analysis to obtain hydrogen depth profiles as a function of time for exposure to water at 90 °C. They observed two sets of diffusion coefficients corresponding to two distinct transport mechanisms. The first, with $D = 10^{-15}$ cm^2/s, was attributed to the rapid diffusion of molecular water into the glass structure. The second, with $D = 6 \times 10^{-18}$ cm^2/s, was associated with the slower breaking of Si–O–Si linkages to form network-terminating silanol groups (SiOH).

In a recent study by Wakabayashi and Tomozawa [27], the diffusion of water into silica was measured in the presence of water vapor at constant temperature for temperatures of 200–750 °C. A time dependent diffusion coefficient was observed for short exposure times and low temperatures which decreased to steady state values. At the same time, the concentration of silanols in the near surface region as measured by FTIR absorption steadily increased. The IR spectrum of surfaces exposed to water at low temperatures showed evidence of hydrogen bonded hydroxyls similar to those found in molecular water. The spectrum of high temperature samples showed no such hydrogen bonding. Two activation energies for steady state diffusion were observed: ~ 80 kJ/mol at temperatures > 550 °C and ~ 40 kJ/mol at lower temperatures (fig. 6). Such behavior suggests that there are two mechanisms for

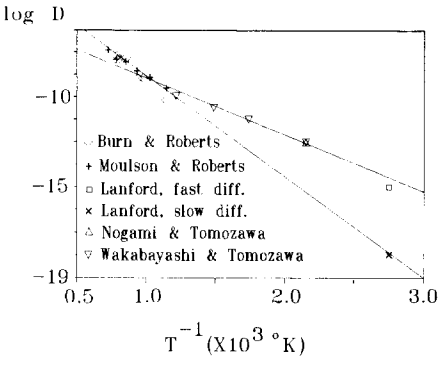

Fig. 6. Diffusion coefficient data for H_2O in silica glass [25–28].

diffusion at any given temperature, in agreement with the conclusions of Lanford et al. [26] but with one mechanism usually dominant. Extrapolation of the lower Arrhenius curve to ambient temperatures gives a good fit to Lanford et al.'s 'fast' diffusion coefficient at 90 °C. Similarly, extension of the upper curve to lower temperatures gives a good estimate of the 'slow' diffusion coefficient at 90 °C.

Nogami and Tomozawa [28] measured water diffusion in silica as a function of hydrostatic pressure and applied uniaxial stress. They observed that the diffusion coefficient increased exponentially with increasing tensile stress and decreased exponentially with increasing compressive stress and hydrostatic pressure. The solubility of water showed an opposite trend. Results for autoclave tests at 192 °C are shown in fig. 7. The diffusion coefficient for zero stress at 192 °C is in excellent agreement with Wakabayashi and Tomozawa's later data for exposure to water vapor (see fig. 6). Their results were explained in terms of the pressure dependent changes in the equilibrium constant in eq. (15) above. For the ideal case, the equilibrium constant K for the reaction may be expressed as

$$K = [\text{Si–OH}]^2/[\text{H}_2\text{O}]. \tag{16}$$

If the activation volume for diffusion V_d is pressure dependent then the effective equilibrium constant at some pressure P may be expressed as

$$K = K_0\, e^{-(V\,dP/RT)}, \tag{17}$$

where K_0 is the equilibrium constant at zero pressure, R is the gas constant, and T is absolute temperature. If the equilibrium constant changes, the apparent diffusion constant also changes in the appropriate direction.

Calculation of the depth below the glass surface to which water diffuses during passage of a polishing particle across the glass surface cannot be done with great precision in the absence of a complete expression for the magnitude of frictional forces. However, a good approximation may be obtained from travelling indenter calculations using coefficients of friction calculated from Amontons law and eq. (9). Appendix 1 summarizes calculations for the case of polishing silica by silica with the following assumptions: a surface temperature of 200 °C, a polishing speed of 5 cm/s, a dwell time at the region of maximum tension equal to the time of particle passage over the surface, and the stress dependence of the water diffusion given by Nogami and Tomozawa [28]. The approximation for the diffusion depth $(2Dt)^{1/2}$ yields a penetration distance for water of 0.5–12 nm depending on particle diameter and pressure as plotted in fig. 8. The calculated diffusion depths are in excellent agreement with measurements showing polishing layer thicknesses to be 1–20 nm in thickness. A typical depth profile of a polished BK7 surface was given by Cook et

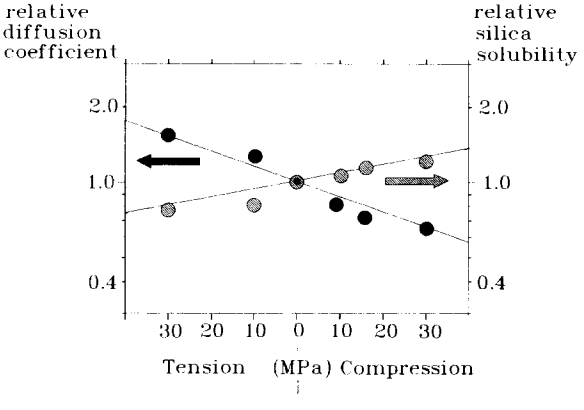

Fig. 7. Diffusion coefficient and solubility of water in silica glass at 192 °C and autogenous pressure (1.21 MPa) as functions of stress. Values normalized to unstressed conditions with $D = 1 \times 10^{-13}$ and solubility 0.9 wt%. (After ref. [28].)

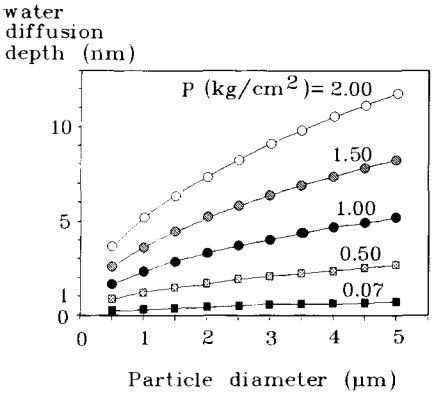

Fig. 8. Calculated water diffusion depths in silica glass vs. silica particle size for various applied pressures from appendix 1.

al. [29] who obtained a layer depth of ~ 17 nm from the half depths of depleted mobile chemical species.

Silica solubility is also a function of particle size. Particles (or surfaces) with a positive radius of curvature have a higher equilibrium solubility, while equilibrium solubility decreases for a negative radius of curvature such as for a crevice or for tangential contact of a particle with a surface. The Ostwald–Freundlich equation gives an expression for the change in solubility [22]:

$$\log_{10}[S/S_i] = 2.85 \times 10^{-7} E_s/Tr, \qquad (18)$$

where S and S_i are the respective solubilities of a surface of radius of curvature r and a planar surface, E_s is the SiO_2/H_2O interfacial surface energy (~ 10 μJ/cm^2) [28], and T is temperature. This relationship is shown graphically in fig. 5(b). The region around the point of contact between a polishing grain and the silica surface is characterized by a small and negative value of r. Hence, the solubility of monomeric silica is expected to be near zero. Ito and Tomozawa [30] proposed that this effect is responsible for the phenomenon of crack tip blunting. Monomeric silica in solution or dissolving from surfaces near the crack tip is precipitated in the region of minimum solubility, thus increasing the radius of curvature at the crack tip. A subsequent publication [31] gave direct evidence for such behavior.

3.2. Aqueous reactions with other glass constituents

It is clear from the results of Izumitani [1,16] (fig. 4) that glass composition and structure can affect polishing rates. Since polishing rates generally increase with decreasing chemical durability and hardness of the corrosion layer, it is appropriate to consider aqueous reactions with other glass constituents.

The initial stage of the reaction of water and a multicomponent silicate glass is exchange of protons or hydronium ions with mobile cations at the glass surface yielding a hydrated silica-rich layer. With time, this exchange becomes diffusion controlled as a concentration gradients move deeper into the bulk from the surface. This exchange process is accompanied by the depolymerization of the siloxane network by water (slow) or by hydroxyl (rapid), together with repolymerization processes. Corrosion of glasses without mobile constituents (e.g. SiO_2) is limited to the network dissolution reactions outlined in the previous section.

For glasses containing alkali ions, the diffusive exchange of alkali into the surrounding water leads to the formation of hydroxyls by

$$R^+(\text{glass}) + H_2O \rightleftarrows H^+(\text{glass}) + ROH, \qquad (19)$$

where R is the mobile alkali cation. The rapid dissociation of ROH causes an instantaneous rise in the local pH of the solution, leading to network dissolution via the reversal of the reaction in eq. (14). Thus the rate of aqueous corrosion is generally proportional to the alkali content of the glass. Moreover, the liquid in the region of the glass surface during polishing will therefore have a somewhat higher pH than the bulk liquid, the difference being determined by the effective alkali flux across the surface and liquid flow at the surface.

While there are abundant data on ionic (e.g. Na^+) and molecular (e.g. He, etc.) diffusion in silicate glasses, data for the diffusion of water in multicomponent silicate glasses are sparse. A recent report by Tomozawa and Tomozawa [32] gives water diffusion rates in a borosilicate glass which are an order of magnitude higher than for vitreous silica. The authors concluded that the

data were in conflict with a molecular transport mechanism and that the rate of transport was influenced by eq. (19) above. The effective diffusion coefficient D_{eff} for water could be expressed as

$$D_{eff} = 2D_m[\equiv Si\text{-}O^-Na^+][H_2O]/[\equiv Si\text{-}OH], \quad (20)$$

where D_m is the molecular water diffusion coefficient. If this is a trend in multicomponent silicates, then water penetration during polishing will always be substantially greater than in vitreous silica, increasing with water content. Interdiffusion of protons and alkali should be also be accelerated in the tensile stress field at the trailing edge of the polishing grain: the magnitude of the stress effect has not been determined.

The consequence of the above processes is that the surface of a multicomponent glass during polishing is expected to develop a hydrated silica surface of greater depth than would vitreous silica under the same conditions. Thus, the polishing particle interacts with a hydrated silica surface whose degree of connectivity is a function of the glass composition, scaling inversely with modifier content and chemical durability, as well as the extent of SiO_2 reprecipitation onto the surface.

The rate of aqueous corrosion of BK7 is $\sim 10^3$ higher than for SiO_2 [24,33]. In contrast, the CeO_2 polishing rate constants for these glasses vary by only a factor of 4. Thus, while polishing rates increase with decreasing chemical durability [1,16] the relationship is relatively weak, suggesting that other processes play a dominant role in determining the rate of surface removal.

3.3. Polishing of silica by silica

The simplest model system for evaluating chemical effects in polishing is the polishing of silica by silica. The only published work for this system is from Izumitani [19]. At pH = 7, 15 nm diameter silica particles polished silica $\sim 40\times$ slower than 1.2 μm diameter CeO_2 but produced $\frac{1}{5}$ the surface roughness. This behavior is consistent with the predicted ratios of surface roughness from eq. (4) above. No polishing was observed in the absence of particles or water. When pH was varied, polishing rates remained constant for pH ≤ 11, but began to increase rapidly for pH ≥ 11 (fig. 9). Even at pH = 14, polishing did not occur in the absence of particles. *

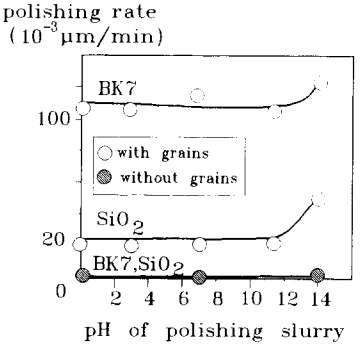

Fig. 9. Polishing rate vs. pH for fused silica and BK7 polished by silica (after ref. [19]).

Izumitani's data for polishing rate vs. pH do not correlate with the change in dissolution rate of SiO_2 with pH [22]. The data do correspond well with pH effects on both surface charge and the polymerization of colloidal silica. The polishing of silica by silica begins to increase rapidly above the maximum pH limit of stability for silica sols, i.e. the pH where dissociation of surface silanol groups approaches 100%. In this regime silica simply dissolves, entering solution as a silicate anion. Thus for the SiO_2/SiO_2 system, depolymerization effects appear to be responsible for increases in the polishing rate. When cerium oxide is used as the polishing compound, dramatically different results are obtained. Both polishing rates and surface smoothness are maximized in the pH range of ~ 9.5–10 [2,4], exactly the range of maximum silica sol stability, where 50% of surface silanols are dissociated.

The polishing rate data given above for pH = 7 translates to the removal of 7 SiO_2 molecules/nm^2 s for polishing of silica by silica and ~ 300 molecules/nm^2 s for ceria polishing as calculated in

* Colloidal silica is also widely used in the semiconductor industry to polish silicon wafers. A number of patented processes exist, all of which employ an operating pH of >10 [34–37]. The Si polishing process is believed to involve the abrasion of an SiO_2 reaction layer.

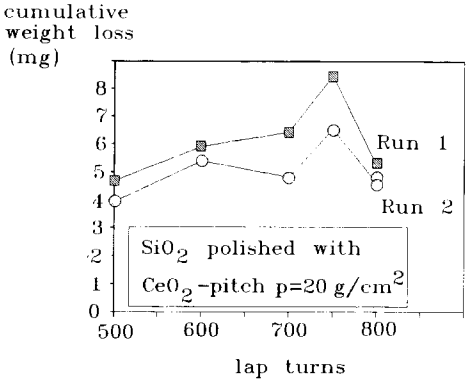

Fig. 10. Weight loss/gain data in silica polishing (after ref. [39]).

Appendix 2. Using the diameters and pressures given in the reference, one may use the set of equations in Appendix 1 to calculate the particle/glass contact area and dwell time to determine the number of particle collisions necessary to remove a molecule from the glass surface. For the polishing of silica by silica, nearly 500 million collisions are required; in striking contrast, only 24 collisions are required to release a silica tetrahedron when polishing with ceria.

3.4. *Deposition effects*

There is experimental evidence for redeposition of material during polishing. Weight gains were repeatedly observed during determination of Preston coefficients for superpolishing of silica glass with fixed-charge cerium oxide laps [38]. These gains occurred at the point at which the polishing particles sank beneath the pitch surface and abrasion ceased. Cumulative weight loss curves for two such polishing runs are given in fig. 10. Examination of the slopes of the curves clearly indicates that the weight gain occurred far more rapidly than the weight loss during polishing. Equivalent rapid weight gains are also observed when glass surfaces begin to lift off the polishing lap, reducing abrasive pressures at the surface and allowing free access of water that contains polishing debris to the freshly formed surface.

Additional indirect evidence for the redeposition of silica may be found in studies of polishing accelerants. Shlishevskii and Migus'kina [39] studied the influence of additives to the polishing liquid. For K8 glass (also known as BK7) the most impressive rate increases were given by 2% solutions of ammonium molybdate. Lesser rate increases were found for Mohr's salt ($(NH_4)_2SO_4 \cdot FeSO_4$) and $ZnSO_4$. Ammonium molybdate is of particular interest since it is well known to form a strong chelation complex with $Si(OH)_4$ but not with silica polymers. It is the reagent of choice for the colorimetric analysis of monomeric silica (the molybdenum blue method) [22]. Iron and zinc salts have been shown to act as precipitants for silica from solution, and adsorb strongly to the silica surface [22,23].

Other chelating agents for monomeric silica have been shown to accelerate glass corrosion. Pyrochatechol, in particular, has been demonstrated both to chelate silica, forming complex anions, and to accelerate its corrosion in neutral and alkaline solutions [22,40]. Chatechols are chemically similar to tannic acid, and are found as products of thermal decomposition of phenolic wood constituents. This is precisely the method by which pitch is produced. Wood flour, particularly walnut flour, is added to polishing pitch as an accelerant [41]. Based on these observations, Brown [42] added varying amounts of catechol to pitch laps, with a resultant increase in the polishing rate of silica.

The only other classes of additives known to accelerate polishing rates are monomers of polishing compounds. Yakovleva et al. [43] found that polishing rates for a number of optical glasses are maximized with additions of zirconium sulphate to the slurry. Similar rate acceleration was observed by Silvernail [44] when $Ce(OH)_4$ was added to a variety of polishing compounds. Of particular interest was the activation of previously inactive oxides (Tb_2O_3, Y_2O_3, Gd_2O_3) by additions of $Ce(OH)_4$. In strong contrast, no activation was obtained when $Si(OH)_4$ is added to the polishing slurry. Kudryavtseva et al. [45] showed that additions of silica to be polishing slurry decreased polishing rates for K8 glass for both CeO_2 and ZrO_2.

Table 1
Summary of data for polishing compounds

Cation	Coord. no.	R–O bond strength (kcal/mol)	IEP [49]	ionic Z/R	Polishing rate [56]	Polishing rate [44]	Rate constant [a] R_c
Ce^{4+}	8	61.4	6.8	4.3	4.9	2.98	0.843
Cr^{3+}	6	41.8	7.4	4.8	3.5	0.59	0.818
Th^{4+}	8	70.1	6.6	3.9			0.691
Fe^{3+}	6	29.5	8.5	3.7	3.1		0.608
Ga^{3+}	6	39.8	8.2 [b]	4.8			0.596
Zr^{4+}	8	62.4	6.2	5.1	2.8	1.62	0.589
Ti^{4+}	6	71.3	6.2	5.9	3.0	1.31	0.569
Sn^{4+}	6	41.8	5.5	5.6	2.5	0.61	0.556
Ni^{2+}	6	17.8	11.0	2.0	1.2		0.544
Zn^{2+}	4	31.5	9.5	3.3	0.9		0.527
Hf^{4+}	8	63.1	5.8	5.1			0.527
In^{3+}	6	33.6	9.4 [b]	3.7			0.524
Mn^{4+}	6	37.3	4.5	4.5	1.5		0.508
Fe^{2+}	6	19.3	12.0	2.6			0.504
Al^{3+}	6	63.2	9.0	5.9	1.8	0.19	0.476
Y^{3+}	6	72.5	9.0	3.2			0.465
αAl^{3+}	6	63.2	9.5				0.455
Sc^{3+}	6	72.6	9.4 [b]	3.7			0.446
Ce^{3+}	6	68.3	9.6 [b]	2.9			0.444
La^{3+}	6	66.7	10.6	2.8			0.420
SiO_2	4	102.5	2.2	9.8	0.01 [c]	0.075 [c]	0.369

[a] $R_c = 1/\log[\text{R–O single bond strength} * \text{abs}(7 - \text{IEP})]$.
[b] Calculated from field strength and eq. 2(b) of ref. [49] ($\text{IEP} = 18.6 - 11.5(Z/R_{\text{eff}})$).
[c] Estimated based on relative rates of CeO_2 vs. SiO_2 polishing from ref. [17] and normalized to CeO_2 data.

3.5. Polishing compounds

Only a few materials act as efficient polishing compounds. For glasses, the best material by far is CeO_2, followed by ZrO_2, ThO_2, TiO_2 and Fe_2O_3. A small number of other oxides are also known to polish glass, but at substantially lower rates. These are summarized in table 1. As discussed above,

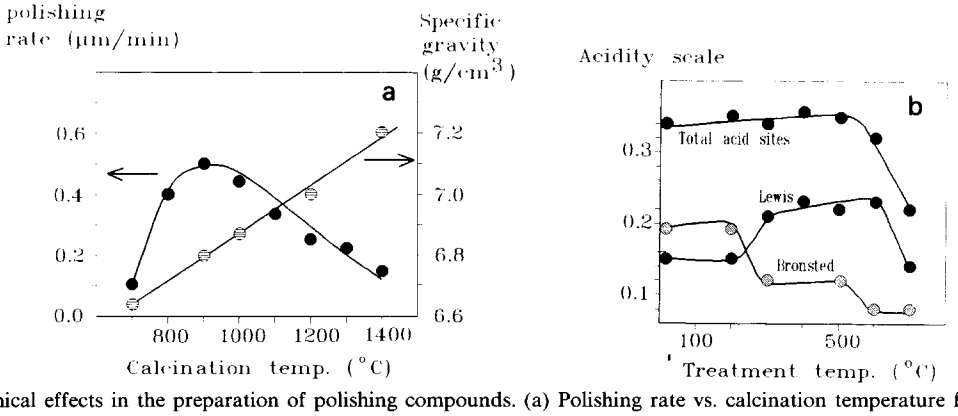

Fig. 11. Chemical effects in the preparation of polishing compounds. (a) Polishing rate vs. calcination temperature for CeO_2 (after ref. [1]). Shaded circles indicate particle density. Closed circles indicate polishing rate. (b) Surface acidity vs. calcination temperature for silica–alumina cracking catalyst (after ref. [47]).

silica has little polishing ability except at very high pH.

Maximum polishing activity is achieved through very specific procedures for preparation of the polishing agents. As reviewed by Izumitani [1] and Silvernail [46], polishing compounds are prepared by precipitation of the hydrous oxide, oxalate, nitrate or carbonate from aqueous solution followed by calcination. Figure 11(a) shows data by Izumitani [1] for CeO_2 indicating that the maximum polishing rate is achieved for a firing temperature of ~ 900 °C. Higher calcination temperatures result in a fully crystalline but less active material. Such methods of preparation and activation maxima with calcination temperature are strikingly similar to those observed for Lewis acid catalysts (electron pair acceptors) (fig. 11(b) [47]). Hertle [48] reported similar behavior for the Lewis acidity of ZrO_2. Maximum Lewis acidity was observed for monoclinic phase, an intermediate phase in the dehydration sequence amorphous-monoclinic-tetragonal. Significantly. Yakovleva et al. [43] reported that the monoclinic phase showed maximum polishing activity. The connection between Lewis acidity and polishing activity is reinforced by the fact that all of the most active polishing agents are strong Lewis acids, a correlation first noted by Brown and Cook [8].

On rehydration, surface hydroxyls are rapidly formed at the Lewis acid sites through dissociative chemisorption. The rate of hydroxyl formation is directly related to the concentration of Lewis acid sites at the surface. Thus, an additional connection between Lewis acidity and polishing activity appears to be the rate of formation and concentration of surface hydroxyls in water. Surface hydroxyl densities [23] for most metal oxides are 5–8/nm^2, similar to the density of silanol groups on the silica surface. The net surface activity of the material will scale with the total number of surface hydroxyls, and therefore its surface area.

The isoelectric point (IEP) of a hydrated oxide surface is defined as the pH at which there is no net surface charge (i.e. when the concentrations of positively and negatively charged species at the surface are equal). The IEP varies as a function of sample preparation, test technique, and the presence of adsorbed surface contaminants. However, the IEP for the hydrated solid oxide surface is generally quite close to pK^1. Parks [49] showed that IEPs for a wide variety of oxides fit an electrostatic model for surface dissociation, with IEP varying inversely with the effective ionic field strength in an aqueous environment Z/R_{eff}, where Z is the cationic charge and R_{eff} is the separation distance between the cation and the adsorbed proton. A summary of IEP values and related properties for silica and polishing compounds is given in table 1. From the above, it is clear that in the pH range used for polishing (7–9), silica, with an IEP ~ 2, has a net negative surface charge, while the surfaces of polishing compounds, particularly CeO_2 and ZrO_2, approach charge neutrality. Thus, the surface of a polishing compound such as CeO_2 is amphoteric, able to adsorb and exchange both cationic (Na^+, Ca^{2+}, etc.) [22–24,

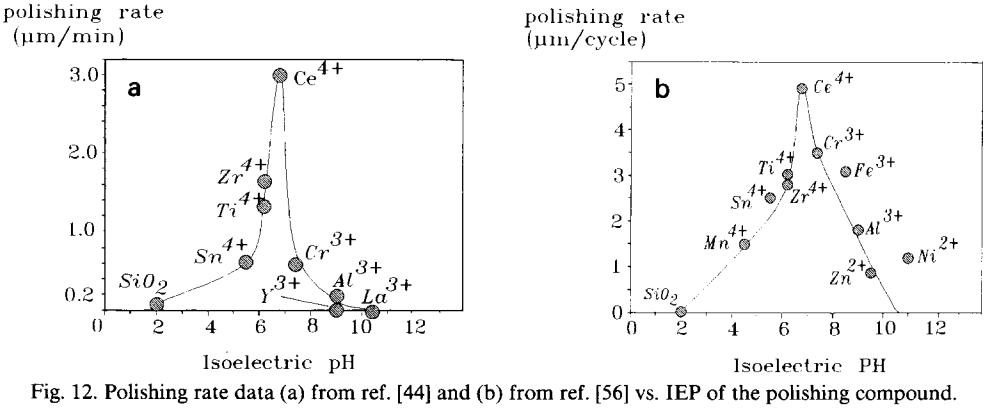

Fig. 12. Polishing rate data (a) from ref. [44] and (b) from ref. [56] vs. IEP of the polishing compound.

50] and anionic (silicate, phosphate, etc.) [22–24, 56]. The total ion-exchange capacity of the polishing grain is a function of its surface area and surface hydroxyl density.

The same behavior holds true for polyvalent metal cations in solution, leading to their strong adsorption at the silica surface over a pH range consistent with their stability. This adsorption and the resultant amphoterism of the surface has been used to explain the ability of such species to precipitate silica colloids from solution [22], suppress aqueous corrosion [22,52,53], and affect static fatigue [54]. On examination, dissolved aquo ions of polishing compounds all bond strongly to the silica surface over a wide pH range so as to reverse the surface charge and precipitate colloidal silica from solution [22]. This ability to precipitate silica from solution as colloidal aggregates may be the basis for activation of the polishing process when salts of the polishing compound are added to the solution. Adsorption of these cations onto multicomponent glass surfaces has also been demonstrated to inhibit alkali transport through the surface [29,55], thus lowering solution pH in the interfacial region.

Relative polishing rates for a variety of compounds on two different glasses [44,56] were examine to obtain further insights into property/polishing rate relationship. * A summary of data is given in table 1.

The variation of the polishing rate with IEP of the polishing compound [49] plotted in figs. 12(a) and (b) is quite pronounced. Maximum polishing rates were obtained at IEP ≈ 7, with rates diminishing at higher and lower values. The rates for silica polishing are extrapolations, and were calculated by dividing the CeO_2 polishing rate by the difference in rates observed by Izumitani [19]; however, they are consistent with the experimental trends. Of the properties examined for trends (coordination number, Gibbs free energy of formation, bond dissociation energy, metal–oxygen single bond strength, aqueous solubility product, Z/R_{ionic}, Z/R_{eff}, pK^1, IEP) only those related to surface charge (pK^1, Z/R_{eff}) or charge density (coordination number) showed correlations with polishing rates. However, a good linear fit to kinetic data was obtained against the inverse logarithm of the product of the oxide single bond strength and the absolute value of the difference of the IEP from the solution pH as seen in figs. 13(a) and (b). Significantly, this calculated rate factor R_c can be used to predict the extent of polishing activity for other oxides. La_2O_3, Ce_2O_3 and Sc_2O_3 should exhibit little polishing activity, while Ga_2O_3 and HfO_2 should have good polishing ability. Of particular interest are the series $Al_2O_3/Ga_2O_3/In_2O_3$ and $TiO_2/ZrO_2/HfO_2$. Predicted polishing rates are $Al_2O_3 < In_2O_3 \ll Ga_2O_3$ and $HfO_2 < TiO_2 < ZrO_2$. Correlation of property trends and polishing rate behavior for these periodic series may give additional insight into the polishing mechanism.

* It should be noted that the properties given are representative of the hydrated oxides and are not those of the materials actually used in the studies cited. Nonetheless they are useful to point out trends.

4. Discussion

The rate of surface removal during polishing is determined by the relative rates of five processes:

(i) the rate of molecular water diffusion into the glass surface;
(ii) subsequent glass dissolution under the load imposed by the polishing particle;
(iii) the adsorption rate of dissolution products onto the surface of the polishing grain;
(iv) the rate of silica redeposition back onto the glass surface;
(v) the aqueous corrosion rate between particle impacts.

The major factors influencing these processes are the load and velocity of the polishing particles, the elastic properties of both glass surface and particle, the chemical durability of the glass, the surface charge of the glass, and the surface charge and ion-exchange capacity of the particle.

For the simplest case, polishing with inert abrasives like diamond, process (iii) is absent. Polishing consists of the passage of a particle under load across the silica (or silicate) surface which produces the following sequence of chemical effects.

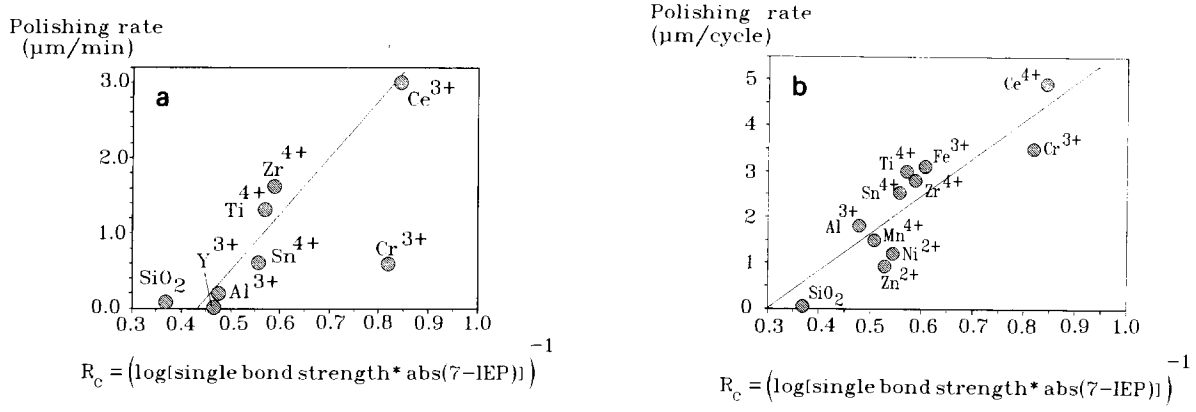

Fig. 13. Polishing rate data from (a) ref. [44] and from (b) ref. [56] vs. R_c.

(1) At the leading edge of the particle, the hydrostatic pressure, elevated liquid temperature and compression forces in the glass surface produce net dissolution of silica, i.e. eq. (15) proceeds in the forward direction to produce solution species ($Si(OH)_4$, $HSiO^{-3}$, etc.) as well as hydroxylated surface species having 1, 2 and 3 remaining linkages to the structural network.

(2) At the trailing edge of the particle, the relief of hydrostatic pressure, combined with strong tensile stresses within the glass surface and the solubility effects of the negative radius of curvature act to precipitate $Si(OH)_4$ released at the leading edge back onto the glass surface. At the same time, molecular water penetrates into the glass surface for some depth. The tensile forces also produce a net reversal of eq. (15), resulting in condensation of silanol groups. The magnitude of the tensile force is determined by the local pressure of the grain.

(3) When the next particle traverses the surface, eq. (15) again proceeds forward, and the interaction continues to depolymerize the network.

Thus, the net effect of the moving polishing grain is to pump water below the glass surface at some steady state depth, and to alternately depolymerize and repolymerize the hydrated silica surface. Net surface removal only results if some $Si(OH)_4$ that is available from depolymerization is removed from the environment or is bound up in some manner. For inactive materials, removal of fully hydrated species from the surface environment depends on turbulence in the liquid. Thus, inactive particles are expected to yield lower polishing rate constants than other polishing materials, in agreement with experimental results for both diamond and boron nitride [10,11].

For the case of chemically active polishing agents such as CeO_2, the magnitude of the tensile force is determined by the local pressure of the grain, the extent of bonding between the particle and the glass surface, and the bond strength of the polishing grain relative to the Si–O bond. Maximum polishing rates are obtained for compounds whose isoelectric pHs are closest to the solution pH, provided that the solution pH is above the IEP of the surface to be polished. Under these conditions, the surfaces of the polishing particles have equal and small concentrations of both positively and negatively charged surface species, the vast majority of the surface hydroxyls being neutral. Evidence given above suggests that the extent of bonding is controlled by a hydrolysis reaction equivalent to eq. (14) above. The rate at which this reaction proceeds is a function of the anion density at the glass surface. A proposed reaction sequence, illustrated in fig. 14, is proposed as follows:

(a) Abstraction of a proton from a hydroxylated silicon-oxygen tetrahedron by a hydroxyl in solution forms a surface Bronsted base ($Si–O^-$) and a water molecule.

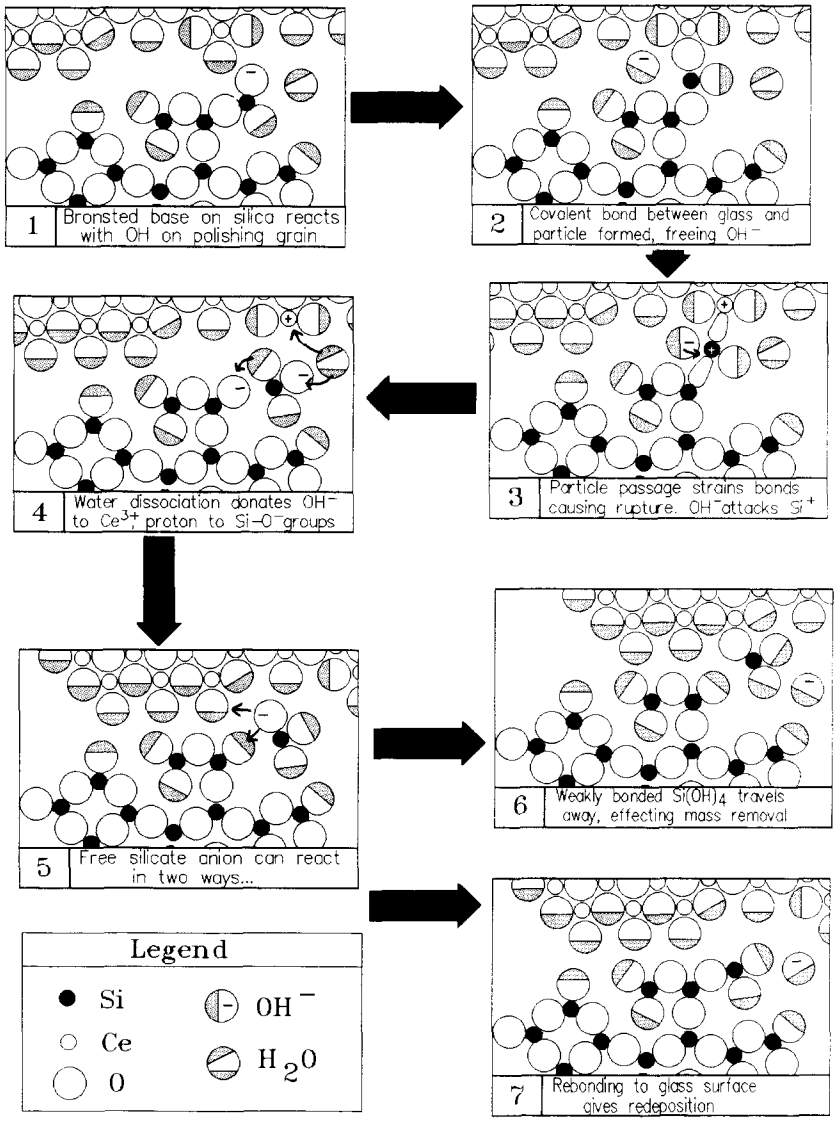

Fig. 14. Proposed polishing reaction sequence.

(b) Reaction of $Si-O^-$ and M–OH sites occurs, releasing a hydroxyl and forming a Si–O–M linkage.

(c) As the particle moves away from the bonding site, the freshly formed Si–O–M bond is strained, leading to bond rupture with several possible outcomes. If the M–O bond strength is lower than that of Si–O, the oxygen will remain with the silicon. Alternatively, if the M–O bond is stronger, the silica tetrahedron will remain bonded to the particle surface, leading to accretion of silica on the particle surface. Strain energies are expected to be insufficient to effect rupture of multiple siloxane linkages. However, for the case of a bonded silica tetrahedron having only one remaining siloxane linkage to the network, elastic recoil and release of strain energy following rupture of the M–O bond can promote scission of this last bridging oxygen of the tetrahedron, releasing a positively charged intermediate species

with the oxygen being retained on the silica surface.

(d) The adjacent molecular water and hydroxyl rapidly react with both the particle surface and the free silica intermediate to reform M–OH on the polishing particle surface and a free silicic acid molecule.

(e) On dissociation, the silicic acid molecule can then rebond to the glass surface, or form a complex with adjacent metal ion sites on the polishing particle surface via hydroxyl exchange. Such anion complexation is most efficient at the pKa of the conjugate acid of the anion [51]. For silicate, this maximum occurs at $pH = -pKa = 9.8$, the pH at which maximum polishing rates with CeO_2 and ZrO_2 are observed. The complexes silicic acid molecule may in turn be displaced by hydroxyl, allowing it to rebond at another surface site, etc. Thus, weakly complexed silicate ions stream off the particle surface into the liquid at the trailing edge of the particle, where they may either repolymerize back onto the glass surface or form colloids in solution.

Scission and release of surface species having only one bridging oxygen linkage initially is considered the most probable processes, as only a single structural linkage must be broken to remove material from the surface. Formation of these species occurs via depolymerization during compression or by aqueous reactions with other glass components (see section 3.2.). Thus, the number of removable surface species, and therefore the polishing rate, should be roughly proportional to the load (eq. (2)), the modifier content of the glass, the rate of aqueous corrosion and surface microhardness, * again in agreement with experimental data.

The above reaction sequence is also consistent with the empirically determined rate factor R_c used to rank relative polishing activity in section 3.5. If both the glass and the polishing particle are the same material, as in the case of silica/silica polishing, contact bonding is inefficient because of the lack of difference in surface charge, and there is no driving force for material removal from the surface due to the equality of bond strengths, i.e. there is equal probability of tetrahedra being removed from the particle surface as there is from the glass surface. Consequently, polishing rates are very low. If the bond strength of the abrasive oxide approaches that of silica, particle accretion occurs because monomers are bound firmly to the particle surface. Too low a bond strength results in the release of insufficient energy upon bond rupture to remove a silica tetrahedron, and yields only weakly bonded surface complexes with silica monomers, allowing rapid back-deposition to the glass surface. Moreover, if the IEP of the polishing particle is far above the solution pH, the particle will simply act as a proton donor to the silica surface, and bonding will not occur. On the other hand, if the IEP is far below the solution pH, the surface hydroxyl concentration will be insufficient for efficient bonding, as in the case of silica/silica polishing.

All of the above discussion on the effects of surface charge has been confined to the silica surface. While it is recognized that the corrosion surface of many silicate glasses is largely hydrated silica, other compositions, particularly aluminosilicates, exhibit IEPs which are substantially higher than silica. Equivalent charge difference effects on polishing rates are expected to apply to these glasses as well, although with a different optimum pH and relative ranking of polishing compounds. Unfortunately, there are virtually no data on surface charge vs. pH and polishing rate data for such glasses, and only limited data on surface composition during aqueous corrosion. Ideal subjects for such investigation are the alkali aluminosilicate pH electrode glasses, whose corrosion chemistry is well understood.

5. Conclusions

Existing models of the mechanics and chemistry of the polishing process have been used to construct a mechanochemical model which, for the first time, predicts the relative polishing activ-

* Microhardness may be defined as the average bond energy per unit volume [57]. This may be reduced by changes in the network density and bonding (hydration and corrosion) or by changes in the surface composition (adsorption, coprecipitation).

ity of compounds as well as the requisite chemical environment at the glass surface for optimal polishing rates. However, a great deal of experimental work remains to validate this model. To date, no polishing studies have adequately characterized the size distribution, surface area and surface activity of the polishing compounds. Such characterization for the series $Al_2O_3/Ga_2O_3/In_2O_3$ and $TiO_2/ZrO_2/HfO_2$ could be combined with polishing rate determinations for well-characterized model glasses over a wide range of solution pH together with compositional depth profiling of the polished surfaces both to verify the model and to extend it. Particular emphasis should be placed on the effects of polyvalent metal glass components, especially Al and Zr, on glass surface charge and polishing rates. In addition, careful study of the rate of silica redeposition will also be required before attempting to develop a quantitative rate model.

There are compelling technical and economic reasons to extend our understanding of the polishing process. Many of the current applications requiring superpolished surfaces have poor yields and stabilities in manufacturing due to inadequate control over the polishing process and a lack of knowledge about the resultant surfaces. In the field of laser ring gyros alone, millions of dollars have been spent on empirical polishing development work in recent years. The model that is presented here suggests polishing rates ~ 10 times higher than currently possible may be achieved by utilizing monosized populations of submicron particulates together with control of silica redeposition, without sacrificing smoothness and introduction of subsurface damage. However such advances will not be possible without additional basic understanding of the polishing mechanism and kinetics.

Appendix 1: Stress and water diffusion for a travelling Hertzian indenter

An example is given of an approximate calculation of the depth to which water diffuses below a glass surface during the polishing of silica by silica (see section 3.1.). The data and formulae used here are drawn from refs. [15] and [28].

Glass: SiO_2
E = Young's modulus = 7.3×10^5 kg/cm^2;
ν = Poisson's ratio = 0.16;
part area $A_p = 5.07$ cm^2 (1 in.^{2}),

Polisher: SiO_2
$E' = 7.3 \times 10^5$ kg/cm^2;
$\nu' = 0.16$.
Grain diameter = $\phi = 3\ \mu m = 3 \times 10^{-4}$ cm;
total load = $L_t = 0.35$ kg;
V = speed = 5 cm/s;
P = pressure = $L_t/A_p = 0.07$ kg/cm^2;
Fill factor = $k = 0.5$ (= 1 for close packed hex);
Temperature at glass surface during polishing = t = 465 K (192° C).

Calculation:
Load per grain
$L = (P/k)\pi(\phi/2)^2 = 9.9 \times 10^{-9}$ kg;
Radius of part/grain contact
$r_c = [(4c_1 l\phi/2)/3E]^{1/3} = 14.6$ nm,
where $c_1 = \frac{9}{16}\{[(1-\nu^2)+(1-\nu'^2)]E/E'\} = 1 \times 10$;
Contact area
$a_c = \pi r_c^2 = 667$ nm^2;
Dwell time of contact
$t_c = 2r_c/V_p = 2.9\ \mu s$;
Mean contact pressure
$p_0 = 1/a_c = 1.5 \times 10^3$ kg/cm^2;
Coefficient of friction
$\mu = (a_c f_b E/10)/1 = 0.49$,
where f_b = fraction of surface area bonded = 0.01;
Maximum surface tensile stress
$\sigma_t = p_0[(1-2\upsilon)/2][1 + c_2\mu] = 2.29 \times 10^3$ kg/cm^2 = 229 mPa,
where $c_2 = [3\pi(4+\upsilon)]/[8(1-2\upsilon)] = 7.207$;
Zero stress diffusion coefficient
$D_0 = 10^{-13}$ cm^2/s;
Activation volume for diffusion
$V_d = 170$ cm^3;
Effective diffusion coefficient
$D_{eff} = D_0\, e^{-(\sigma_t V_d/RT)} = 2.4 \times 10^{-9}$ cm^2/s,
where R is the gas constant;
Time under tensile load = $t_{eff} = 2.9\ \mu s$.

Result:
The diffusion depth for water = $(2D_{eff}t_{eff})^{0.5}$ = 1.2 nm.

Appendix 2: Interaction during the polishing of silica by silica and CeO_2

Examples are given of calculations of the number of collisions needed to remove one molecule of SiO_2 during polishing by SiO_2 and polishing by CeO_2. The source of data and formulae are Izumitani ref. [19] and Appendix 1 of the present paper.

SiO_2 polishing:

Pressure = 0.4 kg/cm^2;
Speed = 5 cm/s;
Particle diameter = 0.015 μm = 1.5×10^{-6} cm.

From appendix 1:

$a_c = 0.054$ nm^2, $p_0 = 2627$ kg/cm^2, $\mu = 0.28$, $\sigma_t =$ 268 mPa, $t_c = 0.005$ μs.
Diffusion depth of water = 0.1 nm.
Observed rate of surface removal
0.02 μm/min = 3.33×10^{-8} cm/s
(Density = $d = 2.2$ g/cm^3, molecular wt. = 60.06 g/mol);
Rate of volumetric surface removal per cm^2 surface area
$r_v = 3.33 \times 10^{-8}$ cm^3/s;
Rate of mass removal
$r_m = r_v d = 7.3 \times 10^{-8}$ g/cm^2 s;
Rate of molecules removed
$r_m/60.06$ g/mol = 1.2×10^{-9} mol/cm^2 s;
Number of molecules removed per unit area and time
$m_r = 1.2 \times 10^{-8}$ mol/cm^2 s $\times 6.023 \times 10^{23}$ molecules/mol
$= 7.4 \times 10^{14}$ molecules/cm^2 s
= 7.4 molecules/nm^2 s.

Result:

Number of molecules removed per particle impact $m_r t_c a_c = 2 \times 10^{-9}$ molecules per impact, or 1 SiO_2 molecule is removed for every 500 million collisions.

CeO_2 polishing:

Pressure = 0.4 kg/cm^2;
Speed = 5 cm/s;
Particle diameter = 1.2 μm = 1.2×10^{-4} cm.

From appendix 1:

$a_c = 337$ nm^2;
$p_0 = 2684$ kg/cm^2;
$\mu = 0.27$,
$\sigma_t = 270$ mPa;
$t_c = 0.4$ μs;
Diffusion depth of water = 1.1 nm.
Observed rate of surface removal
0.82 μm/min = 1.37×10^{-6} cm/s,
(Density = $d = 2.204$ g/cm^3, molecular wt. = 60.06 g/mol);
Rate of volumetric surface removal per cm^2 surface area
$r_v = 1.37 \times 10^{-6}$ cm^3/s;
Rate of mass removal
$r_m = r_v d = 3 \times 10^{-6}$ g/cm^2 s;
Rate of molecules removed
$r_m/60.06$ g/mol = 5×10^{-8} mol/cm^2 s;
Number of molecules removed per unit area and time
$m_r = 5 \times 10^{-8}$ mol/cm^2 s $\times 6.023 \times 10^{23}$ molecules/mol
$= 3 \times 10^{16}$ molecules/cm^2 s
= 300 molecules/nm^2 s.

Result:

Number of molecules removed per particle impact $m_r t_c a_c = 0.04$ molecules per impact, or
1 SiO_2 molecules removed for every 24 collisions.

References

[1] T. Izumitani, in: Treatise on Material Science and Technology, Vol. 17, eds. M. Tomozawa and R. Doremus (Academic Press, New York, 1979) p. 115.
[2] L. Holland, The Properties of Glass Surfaces (Chapman and Hall, London, 1964).
[3] F. Preston, J. Soc. Glass Tech. 11 (1927) 214.
[4] N. Brown, Document MISC4476 (Lawrence Livermore National Laboratory, Livermore, CA 1987).
[5] W. Silvernail, Optical World 9 (1980) 7.
[6] N. Brown, Ann. Rev. Mater. Sci. 16 (1986) 371.
[7] N. Brown, P. Baker and R. Maney, Proc SPIE 306 (1981) 42.
[8] N. Brown and L. Cook, Paper TuB-A4, Tech. Digest, Topical Meeting on the Science of Polishing, Optical Society of America, 17 April 1984.
[9] N. Brown, Precision Engineering 9 (1987) 129.

[10] N. Brown and B. Fuchs, Optical Fabrication and Testing 1988 Digest Series, 13, Optical Society of America, 4 Nov. 1988.
[11] N. Brown and B. Fuchs, Ductile grinding of glass, unpublished manuscript (1989).
[12] Y. Namba, Paper TuB-A2, Tech. Digest, Topical Meeting on the Science of Polishing, Optical Society of America, 17 April 1984.
[13] Y. Morii, K. Yamauchi and K. Endo, Precision Engineering 9 (1987) 123.
[14] Y. Morii, K. Yamauchi and K. Endo, Precision Engineering 10 (1988) 24.
[15] B. Lawn and R. Wilshaw, J. Mater. Sci. 10 (1975) 1049.
[16] T. Izumitani, Paper MA1, Techn. Digest, Topical Meeting on Optical Fabrication and Technology, Optical Society of America, 1982.
[17] R. Bartholemew, J. Non-Cryst. Solids 56 (1983) 331.
[18] M. Tomozawa, in: Proc. 7th Int. Conf. on Fracture, eds. K. Salamana et al. (Pergamon, New York, 1989) p. 1566.
[19] T. Izumitani, Paper TuB-A1, Tech. Digest, Topical Meeting on the Science of Polishing, Optical Society of America, 17 April 1984.
[20] D. Cornish and L. Watt, Br. Sci. Instr. Res. Assoc. Rep. R295 (1963).
[21] W. Silvernail and N. Goetzinger, Glass Ind. 52 (1971) 130.
[22] R. Iler, The Chemistry of Silica (Wiley, New York, 1979).
[23] P. Schindler, in: Adsorption of Inorganics at Solid–Liquid Interfaces, eds. M. Anderson and A. Rubin (Ann Arbor Science, Ann Arbor, 1981) p. 1.
[24] R. Doremus, Glass Science (Wiley, New York, 1973) chs. 8 and 9.
[25] M. Nogami and M. Tomozawa, Phys. Chem. Glasses 25 (1984) 82.
[26] W. Lanford, C. Burman and R. Doremus, in: Advances in Materials Characterization II, eds. R. Snyder, R. Condrate and P. Johnson (Plenum, New York, 1985) p. 203.
[27] H. Wakabayashi and M. Tomozawa, J. Am. Ceram. Soc. 72 (1989) 1850.
[28] M. Nogami and M. Tomozawa, J. Am. Ceram. Soc. 67 (1984) 151.
[29] L. Cook, A. Marker, K.-H. Mader, H. Bach and H. Müller, Glastech. Ber. 60 (1987) 302.
[30] S. Ito and M. Tomozawa, J. Am. Ceram. Soc. 65 (1982) 368.
[31] Y. Bando, S. Ito and M. Tomozawa, J. Am. Ceram. Soc. 67 (1984) C-36.
[32] H. Tomozawa and M. Tomozawa, J. Non-Cryst. Solids 109 (1989) 311.
[33] L. Cook and K.-H. Mader, Glastech. Ber. 60 (1987) 333.
[34] R. Walsh and A. Herzog, US Patent no. 3,170,273 (1965).
[35] B. Tredinnick, R. Gambale and P. Dupree, US patent no. 3,715,842 (1973).
[36] W. Cromwell, US patent no. 3,807,979 (1974).
[37] G. Sears, US patent no. 3,922,393 (1975).
[38] N. Brown, private communication (1989).
[39] B. Shlishevskii and Z. Migus'kina, Sov. J. Opt. Technol. 44 (1977) 680.
[40] F. Ernsberger, J. Am. Ceram. Soc. 42 (1959) 373.
[41] A. Franks, Mater. Sci. Eng. 19 (1975) 169.
[42] N. Brown, private communication (1985).
[43] T. Yakovleva, L. Chunyayeva, A. Kovalenko and B. Belyavskaya, Sov. J. Opt. Technol. 41 (1974) 44.
[44] W. Silvernail, Paper WB1-1, Techn. Digest, Topical Meeting on Optical Fabrication and Technology, Optical Society of America, 1982.
[45] N. Kudryavtseva, T. Yakovleva and G. Khodakov, Sov. J. Opt. Technol. 46 (1979) 223.
[46] W. Silvernail, Paper TuB-B1, Tech. Digest, Topical Meeting on the Science of Polishing, Optical Society of America, 17 April 1984.
[47] K. Bourne, F. Cannings and R. Pitkethley, J. Phys. Chem. 74 (1970) 2197.
[48] W. Hertl, Langmuir 5 (1989) 96.
[49] G. Parks, Chem. Rev. 65 (1965) 177.
[50] D. Kinniburgh and M. Jackson, in: Adsorption of Inorganics at Solid–Liquid Interfaces, eds. M. Anderson and A. Rubin (Ann Arbor Science, Ann Arbor, 1981) p. 91.
[51] F. Hingston, in: Adsorption of Inorganics at Solid–Liquid Interfaces, eds. M. Anderson and A. Rubin (Ann Arbor Science, Ann Arbor, 1981) p. 51.
[52] L. Cook, Glastech. Ber. 60 (1987) 368.
[53] C. Das, J. Am. Ceram. Soc. 64 (1981) 188.
[54] P. Fox, Phys. Chem. Glasses 21 (1980) 161.
[55] J. Tait and C. Jensen, J. Non-Cryst. Solids 49 (1982) 363.
[56] A. Kaller, Mschr. Feinmech. Opt. 79 (1962) 135.
[57] J. Plendl and P. Gielesse, Phys. Rev. 125 (1962) 828.